Elastic-wave propagation through disordered and/or absorptive layered systems

M. M. Sigalas and C. M. Soukoulis
Ames Laboratory and Department of Physics and Astronomy, Iowa State University, Ames, Iowa 50011
(Received 9 September 1994)

Using the transfer-matrix method, we study the propagation of elastic waves through disordered solid multilayers constructed from two different materials and assumed periodic on the average. Results for different incident angles are reported; the effect of the mixing between longitudinal and transverse type of waves in the case of incident angles different from normal is discussed. We also study absorbing systems and how the localization length changes in the presence of dissipation.

I. INTRODUCTION

In the last few years the problem of classical wave (CW)—such as electromagnetic (EM), acoustic, or elastic (EL)—propagation in disordered systems has received increasing interest.[1–3] It has been pointed out[3] that there is a connection between the possible localization of CW in disordered media and the possible existence of band gaps or regions of very low density of states in periodic structures. Actually, the band gaps will become, at least partially, regions of localized states as a disordering process is gradually introduced in a periodic structure; in addition; those localized states are expected to have smaller localization lengths, so, they can be verified more easily experimentally. For that reason, considerable effort has been focused in the study of disordered systems that are periodic on the average. In particular, there are some recent theoretical works concerning the study of EM waves in one-dimensional (1D) disordered systems that are periodic on the average,[4–7] but there is still no conclusive experimental evidence on that subject.

In the present work we study the propagation of elastic waves in 1D systems. There has been extensive theoretical studies on EL wave propagation in multilayered media for more than 50 years,[8–18] since it is important in many scientific areas such as seismology, nondestructive evaluation, design of acoustic devices, etc. However, there are still open questions, such as, what is the effect of the disorder and/or the absorption in the propagation of elastic waves through multilayered media that are perturbed from the periodicity, which we are dealing with in the present work. The transfer-matrix method (Sec. II), proposed recently by Munjal,[14] has been used for the calculation of the transmission properties of the composite multilayers. Since our starting point is a periodic multilayer, it is important to understand their properties (Sec. III). Most of the recent numerical simulations have focused on the transmission and reflection properties of periodic multilayers for normal incidence waves;[12–18] in that case only longitudinal (L) or transverse (T) waves are excited in the solid layers; in the present work, we also study incident angles different from normal, where both L and T waves are excited and mixed together, and how this affects the transmission. Defects introduced in the periodic multilayers are also studied (Sec. IV) and their possible applications in the design of acoustical filters are discussed. The localization of elastic waves in disordered multilayers is also studied (Sec. V) and the results are compared with the corresponding case of the electromagnetic wave propagation through dielectric multilayers.[4–7] Finally, absorbing multilayers are studied (Sec. VI) and the effect of the absorption in the localization length is discussed.

II. THEORY

When a plane wave of frequency ω and propagating in the x,y plane, is incident on a plate with an angle θ relative to the y axis, it induces a normal stress σ_y and a shear stress τ_{xy} in a plate and those two stresses are accompanied by a normal particle velocity v_y and tangential velocity v_x. In the cases of electromagnetic waves propagating through dielectric multilayers or acoustic waves propagating through fluid multilayers, there is only one type of wave and the corresponding transfer matrix is a 2×2 matrix. But, solid layers can sustain both L and T waves, so a 4×4 matrix is needed in this case.

In the present work, we follow the formalism described recently by Munjal,[14] in which the vector consisting of the four state variables at the end of the plate,

$$F(h)=[\sigma_y(h),\tau_{xy}(h),v_x(h),v_y(h)]^T$$

(where the superscript T means the transpose of a vector), is connected with the vector $F(0)$ at the beginning of the plate, by the following relation:

$$F(0)=MF(h)\ . \tag{1}$$

Here M is the 4×4 transfer matrix given in Eq. (22) of Ref. 14. For a certain plate, the transfer matrix can be defined from the T and L sound velocities, c_L,c_T, the density ρ, the thickness of the plate h, the incident angle θ, and the frequency ω of the incident plane wave. The total transfer matrix of a multilayer can be found by multiplying M for each layer, so the state variables at the end of the multilayer can be connected with those at the beginning of the slab. For normal incidence, the 4×4 transfer matrix can be separated into two uncoupled 2×2 transfer matrices, one for the transverse and one for the longitudinal waves.

0163-1829/95/51(5)/2780(10)/$06.00 ©1995 The American Physical Society

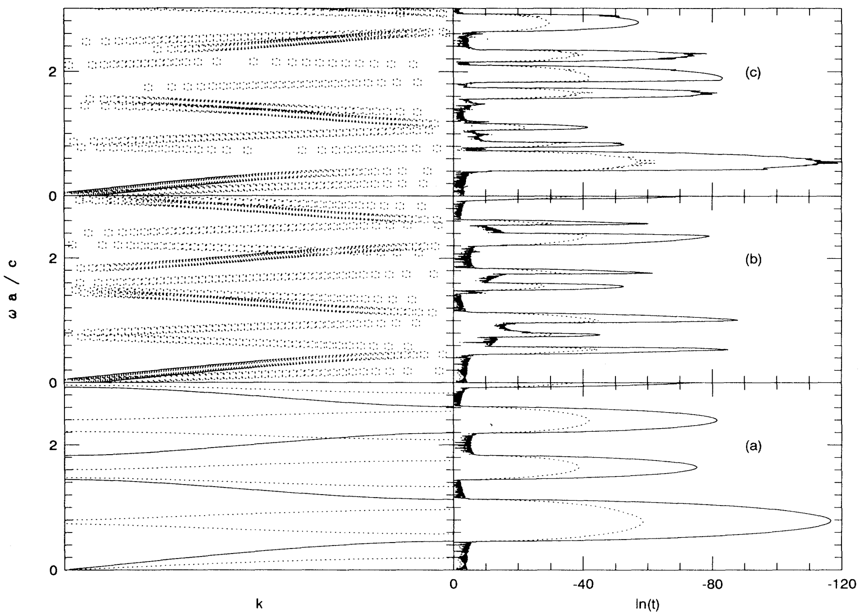

FIG. 1. The band structure (left panels) and the transmission profiles (right panels) for elastic waves propagating through a periodic bilayer consisting of equal thickness steel and lucite plates; the incident angles are 0° (a), 5° (b), and 45° (c); the transmission is calculated for 20 and 40 bilayers (dotted and solid lines in right panels).

For the case where the ambient media are the same inviscid fluid, $\tau_{xy}=0$ at the exposed surfaces and the reflection r and the transmission t coefficients are[14]

$$r=|(A-ZB)/(A+ZB)|^2 , \tag{2}$$

$$t=|2ZM_{23}/(A+ZB)|^2 , \tag{3}$$

where

$$A=M_{13}(M_{21}Z+M_{24})-M_{23}(M_{11}Z+M_{14}) , \tag{4}$$

$$B=M_{43}(M_{21}Z+M_{24})-M_{23}(M_{41}Z+M_{44}) , \tag{5}$$

$$Z=\rho c/\cos\theta . \tag{6}$$

ρ, c are the density and sound velocity in the ambient media, respectively, and M_{ij} are the matrix elements of the total transfer matrix M. Assuming that c_a is the absorption coefficient, the following relation must hold: $r+t+c_a=1$.

III. PERIODIC MULTILAYERS

The left panels of Fig. 1 show the band structure of an infinite periodic bilayer system consisting of steel and lucite plates of equal thickness; the sound velocities and densities of the materials are given in Table I. For normal incidence ($\theta=0°$), the T and L modes [dotted and solid lines in left panel of Fig. 1(a)] are uncoupled. Because of the high velocity contrast between steel and lucite, there are wide gaps for both modes; in particular, the first gap has ratio of gap over midgap frequency $\Delta\omega/\omega_g=0.843, 0.991$ for the L and T modes, respectively.

The band structure for $\theta=5°$ [left panel of Fig. 1(b)] is almost the same with that for $\theta=0°$, but, in that case as well as for every $\theta\neq 0°$, there is always a mixing between the two type of waves, so, we cannot distinguish the T from the L modes. The first gap between the second and third bands [see left panel of Fig. 1(b)] is very small ($\Delta\omega/\omega_g=0.323$). By increasing the incident angle the third band tends to higher frequencies (especially for k points close to the edge of the Brillouin zone), while the second band remains almost unchanged, so, the first gap increases as θ increases [compare the left panels of Figs. 1(b) and 1(c)]; in particular, $\Delta\omega/\omega_g=0.466, 0.614, 0.772$ for $\theta=30°, 45°, 60°$, respectively.

The right panels of Fig. 1 show the transmission versus $\omega a/c$ for a finite thickness periodic multilayer consisting of equal thickness steel and lucite plates embedded in water; a is the thickness of one bilayer and c is the longitudinal sound velocity of lucite. For $\theta=0°$ [Fig. 1(a)], only the longitudinal modes are excited, so, there are three drops in the transmission corresponding to the three gaps which appear in the band structure of the longitudinal modes. But, the transmission changes drastically even for small deviations from normal incidence because of the mixing of the L and T modes. This is clearly shown by comparing the transmission for $\theta=0°$ and 5° [right panels in Figs. 1(a) and 1(b)]; for $\theta=0°$, the transmission at $\omega a/c=0.459$ and 1.128 (the edges of the first gap for $\theta=0°$) is almost identical with that for $\theta=5°$, but there is now transmission around $\omega a/c=0.6$ and 0.9 due to the second and third T-type bands.

TABLE I. The Young modulus E, Poisson's ratio σ, and density ρ, and the longitudinal c_L, and transverse c_T, sound velocities for the materials used in the present work (Refs. 20 and 21).

Material	E (kbar)	σ	ρ (gm/cm^3)	c_L (km/sec)	c_T (km/sec)
Lucite	400	0.400	1.18	8.57	3.50
Al	774	0.353	2.73	6.79	3.24
Cd	756	0.283	8.75	3.33	1.83
Si	1627	0.223	2.33	8.94	5.34
Steel	1960	0.300	7.89	5.78	3.09

A common feature of the transmission for frequencies inside the gaps is the dependence of the $\ln(t)$ on the thickness of the system, Λ; in particular, for $\theta=0°$ and $\omega a/c=0.8$, $\ln(t)$ is -116 and -56 for $\Lambda/a=40$ and 20, respectively (a is the thickness of one bilayer). So, it turns out that for frequencies inside the gaps, $\ln(t)$ is proportional to $-\Lambda$, while for frequencies outside of gaps the transmission is almost constant (it actually oscillates around a constant value as Λ increases due to the multiple scattering from the two boundary sides of the system).

The band structure changes as the ratio of the thickness of steel (h_S) and lucite (h_L) layers changes. In particular, for $h_S/h_L=3$ and $\theta=0°$ (see Fig. 2), the ratio $\Delta\omega/\omega_g=0.548$, 0.726 for the first gap of the L and T modes, respectively, which are smaller than those for $h_S/h_L=1$. But, most interestingly, for $h_S/h_L=3$, the second gap of the T modes (dotted lines in Fig. 2) between $\omega a/c=0.904$ and 0.568 almost coincides with the first gap of the L modes (solid lines in Fig. 2) which is located between $\omega a/c=0.859$ and 0.489. So, this gap survives even for small deviations from normal incidence; in particular, the upper edge of this gap (at $\omega a/c=0.859$) remains at almost the same frequency for angles as high as 45° while the lower edge moves to higher frequencies (the lower edge of this gap is at $\omega a/c=0.614$ for $\theta=45°$). Multilayers with that feature can be used as high reflection devices or wide stop-band filters operating in a wide range of angles. By even increasing the incident angle, the second T-type band moves to higher frequencies remaining almost flat, while the third T-type band remains almost unchanged, so, the gap tends to disappear.

IV. DEFECTS

Defects can be created by changing (a) the sequence of the layers, (b) the thickness of the layers, (c) the material properties of one of the layers. Regardless of the defect's type, its result is basically the creation of states well localized around the defect region and at frequencies inside the gaps of the periodic case. In the present work, we use the first type of defect; in particular, assuming a system of N layers with an AB stacking sequence, we change the sequence of the layers (from AB to BA) after the $N/2$ layer. The A and B are steel and lucite plates and $N=10$. For normal incidence and equal thickness layers [see solid line in Fig. 3(a)], a very sharp peak in the transmission appears at $\omega a/c=0.723$. The sharpness of the peak is measured by the quality factor $Q=\omega_d/(\omega_1-\omega_2)$, where ω_d is the frequency at the top of the peak and ω_1,ω_2 are the frequencies below and above ω_d where the transmission is 3 dB less than that at the top of the peak. Q depends strongly on the number of the bilayers; in particular, Q is 2.4×10^5, 3.3×10^4, 1.8×10^3, 1.1×10^2 for 10, 8, 6, 4 bilayers, respectively; in all the cases the transmission at the top of the peak is practically 1 (all the power is transmitted), while the ω_d slightly moves to smaller frequencies as the number of bilayers decreases (the difference of the $\omega a/c$ between 10 and 4 bilayers is 0.01). As in the case of dielectric multilayers, such kinds of systems can be used for the development of narrow band-pass filters. It will be also interesting if those peaks in the transmission survives for incident angles different from normal. But, this does not happen for $h_S/h_L=1$. For $\theta=10°$ [dotted line in Fig. 3(a)], the peak in the transmission due to the defect has almost disappeared because in that frequency region there is now transmission due to the second and third T-type bands lying inside the first gap of the L-type modes (see Fig. 1). In contrast, for $h_S/h_L=3$ [Fig. 3(b)], the peak is almost the same for $\theta=0°$ (solid line) and 10° (dotted line). There is a slight shift of the peak towards higher frequencies as the incident angle increases, while the value of Q is almost the

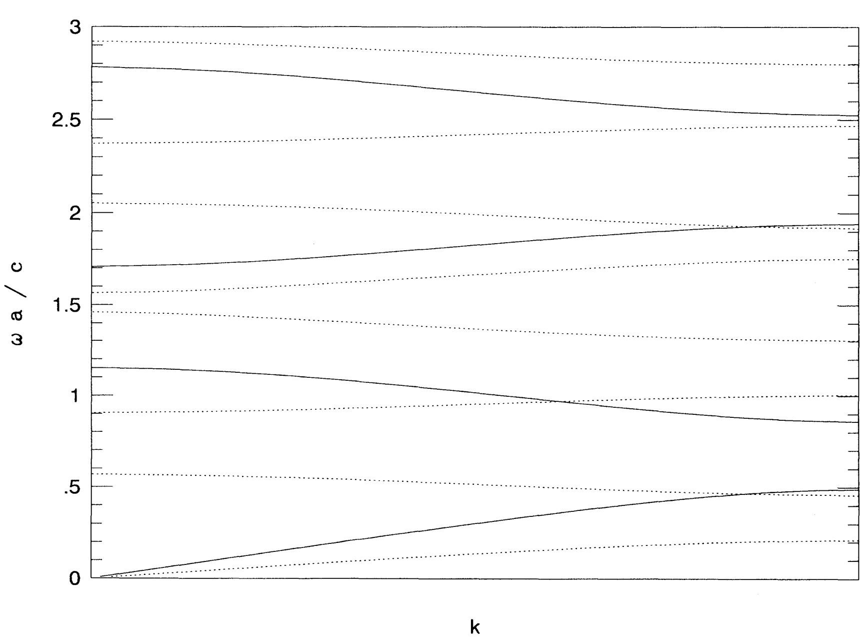

FIG. 2. The band structure of elastic waves propagating through a bilayer consisting of steel and lucite plates; the thickness of the steel plate is three times the thickness of the lucite plate and the incident angle is 0°.

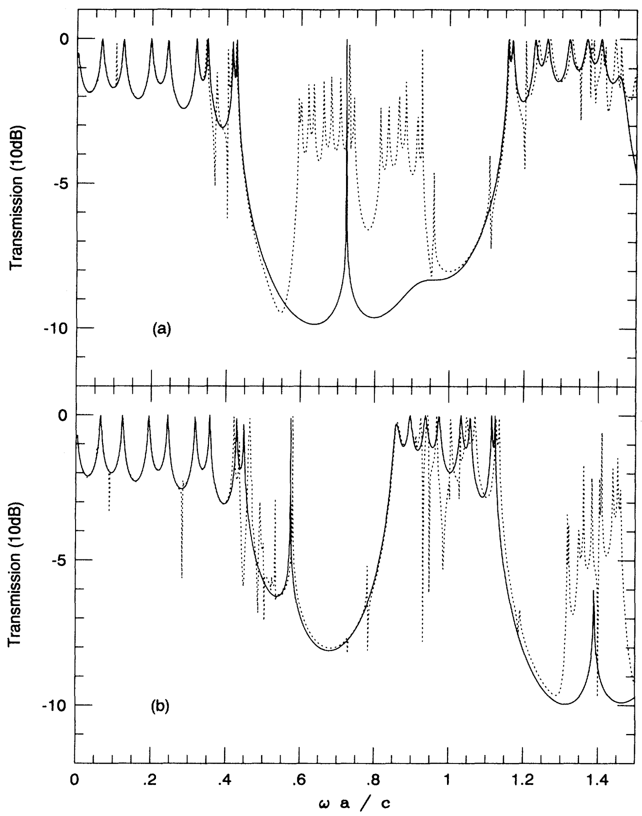

FIG. 3. The transmission vs frequency for a 10-bilayer system with a defect (see text) for incident angles 0° and 10° (solid and dotted lines). The thickness ratio between steel and lucite plates is $h_S/h_L=1$ and 3 (upper and lower panels, respectively).

same ($\omega_d a/c=0.575$, 0.580, 0.597, and 0.619 for $\theta=0°$, 10°, 20°, and 30°, respectively). There are also some smaller peaks close to the lower edge of the gap due to the second T-type band.

V. DISORDER

It is well known that waves propagating through one-dimensional (1D) disordered media are always localized. This implies that the transmission t is given by

$$\langle \ln(t) \rangle = -\frac{2\Lambda}{l} , \tag{7}$$

where l is the so-called localization length, Λ is the thickness of the multilayer and $\langle \cdots \rangle$ represents an average over the statistical distribution of the randomness. $\langle \ln(t) \rangle$ and l depend on the materials constructed the multilayer, the amount of disorder, the frequency, and the incidence angle; it is the purpose of the present study to investigate the influence of those factors on $\langle \ln(t) \rangle$ and l.

In all the following cases, we study multilayers consisting of two materials with an AB stacking sequence and embedded in water. The thickness of the ith layer is given by $d_i=(1+\gamma_i)a/2$, where $a/2$ is the average thickness of each layer and γ_i is randomly distributed over the interval $[-d,d]$; the thickness error is defined by the percentage difference between d and $a/2$. The $\langle \ln(t) \rangle$ is calculated by finding the logarithmic average over 100 configurations and assuming a flat statistical distribution.

Figure 4 shows the $\langle \ln(t) \rangle$ for a 40-bilayer system consisting of steel and lucite plates assuming 40% error in the thickness of each layer. The $\langle \ln(t) \rangle$ obeys the relation described by Eq. (7) for every incident angle and frequency with the only exception being frequencies which are close to zero. This is expected, since, as ω tends to zero, the wavelength increases, so, the wave is not affected from the variations of the structure, but it actually "sees" an homogeneous effective medium.[5] The large drops in the average transmittance in moderate frequencies correspond to the first gap of the corresponding periodic cases (see Fig. 1), while all the higher gaps of the periodic case have almost disappeared; there is only a much smaller drop of the $\langle \ln(t) \rangle$ at around $\omega a/c=2.7$ for both $\theta=0°$ and 5° which is reminiscent of the corresponding gap of the periodic case (compare with the transmission in Fig. 1). For $\theta=0°$, the $\langle \ln(t) \rangle$ in the middle of the first drop ($\omega a/c=0.75$) is actually higher than the $\ln(t)$ of the periodic case due to the fact that the density of states (DOS) is higher in the disorder case because of the

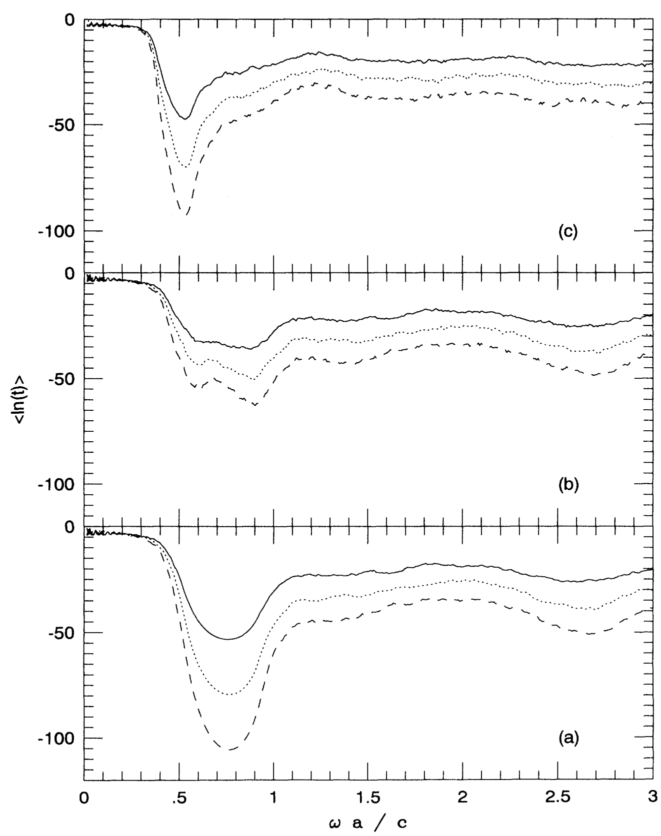

FIG. 4. The logarithmic average of the transmission vs frequency for 20, 30, and 40 bilayers (solid, dotted, and dashed lines) disordered system consisting of equal on the average thickness steel and lucite plates; each layer has a 40% error thickness, $\langle \ln(t) \rangle$ is calculated making an average over 100 configurations and the incident angle is $\theta=0°$ (a), 5° (b), and 45° (c).

creation of localized states inside the gap.[4,5] For $\theta=5°$, the average transmission inside the first gap is even higher because in that case the T-type modes are also excited so the DOS is even higher; note that there is also a small peak in the average transmission at $\omega a/c=0.7$, which comes from the second and third T-type bands in the periodic case [see Figs. 1(a) and 1(b)]. At high frequencies, the $\langle \ln(t) \rangle$ saturates to an almost constant value; using that saturated value, we can find from Eq. (7) that the localization length is almost equal with the average thickness of two bilayers. At high frequencies (small wavelengths) the phase coherence between the scattering at different interfaces is lost and the dominant factor is the scattering from each interface; but, the transmission and reflection coefficients at a sharp interface are frequency independent; for that reason the $\langle \ln(t) \rangle$ and l are also frequency independent at high frequencies.[5]

Although $\langle \ln(t) \rangle$ obeys Eq. (7) as we discussed in the previous paragraph, the $\ln(t)$ fluctuates from its average value depending on the particular configuration. Figure 5 shows $\ln(t)$ vs the frequency for a 40-bilayer system consisting of steel and lucite for one of the configurations used in the calculation of $\langle \ln(t) \rangle$ in Fig. 4(c); the thickness error is 40% for each layer and the incident angle is $\theta=45°$. There are two sharp peaks in the transmission at $\omega a/c=0.943$ and 2.681; the quality factor for that peak is extremely high (higher than 10^6), while at the top of those peaks a substantial percentage of the power is transmitted (especially for the first peak the transmission is almost 1). In order to find those peaks, the frequency step close to the peaks was two order of magnitudes smaller than the usual step (as a result of the extremely high Q), so, some additional peaks might be lost. There are also frequencies where $\ln(t)$ is much smaller than its average value; for example, $\ln(t)=-62$ at $\omega a/c=1.68$, while its average value at the same frequency is -38.

The localization length depends on the amount of the disorder. Figure 6 show the $\langle \ln(t) \rangle$ vs $\omega a/c$ of a 40-bilayer system consisting of steel and lucite plates with equal, on the average, thickness; the incident angle is 0° although the conclusions are the same for all incidence angles; the thickness error of each plate is 20, 40, and 80%. For the 20% case (solid line in Fig. 6), there are two sharp drops in the $\langle \ln(t) \rangle$ around $\omega a/c=0.75$ and 1.65 which are reminiscent of the first and second gaps of the corresponding periodic case. By increasing the disorder, those drops (especially the high-frequency ones) tend to disappear and $\langle \ln(t) \rangle$ saturates to an almost constant value (-40, which corresponds to a localization length of almost two unit cells) independent of frequency. This is in accordance with the previously studied case of electromagnetic waves propagating through 1D disordered media.[4,5] In general, $\langle \ln(t) \rangle$ decreases by increasing the amount of disorder; e.g., for $\omega a/c=2$ and $\theta=0°$, $\langle \ln(t) \rangle$ is -24, -35, -55 (Fig. 6) for thickness error 20, 40, and 80%, respectively. However, there are frequency regions where $\langle \ln(t) \rangle$ increases by increasing the disorder; e.g., for frequencies inside the first gap of the periodic case at around $\omega a/c=0.75$ (see Fig. 6), $\langle \ln(t) \rangle$ is -114, -106, and -67 for thickness error 20, 40, and 80%, respectively. As we explained previously, this is because the DOS in that region increases by increasing the disorder.

In a periodic case, the position and the width of the gaps are strongly related to the ratios of densities r_ρ, and sound velocities r_L and r_T between the two materials consisting the multilayer. We expect that there will be also a similar strong dependence in a disordered multilayer. Figure 7 shows $\langle \ln(t) \rangle$ vs $\omega a/c$ for a 40-bilayer system consisting of plates which have equal thickness on the average for the two different materials; the incident angle is $\theta=45°$ and the error in the thickness of each layer is 40%. In all the cases, one of the plates is lucite while the other is either Al, Si or Cd; the parameters for each ma-

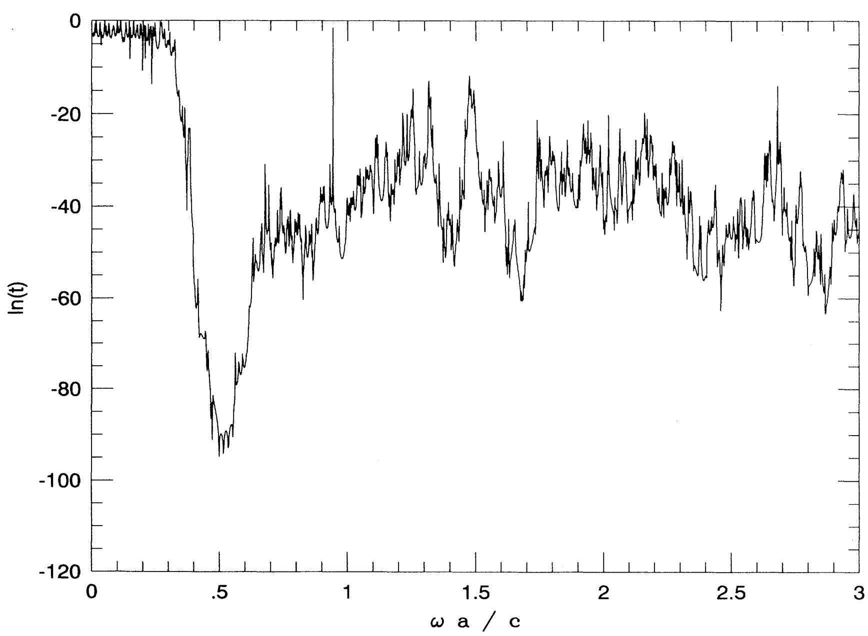

FIG. 5. The transmission vs frequency for one of the configurations used in Fig. 4 and a system consisting of 40 bilayers with $\theta=45°$.

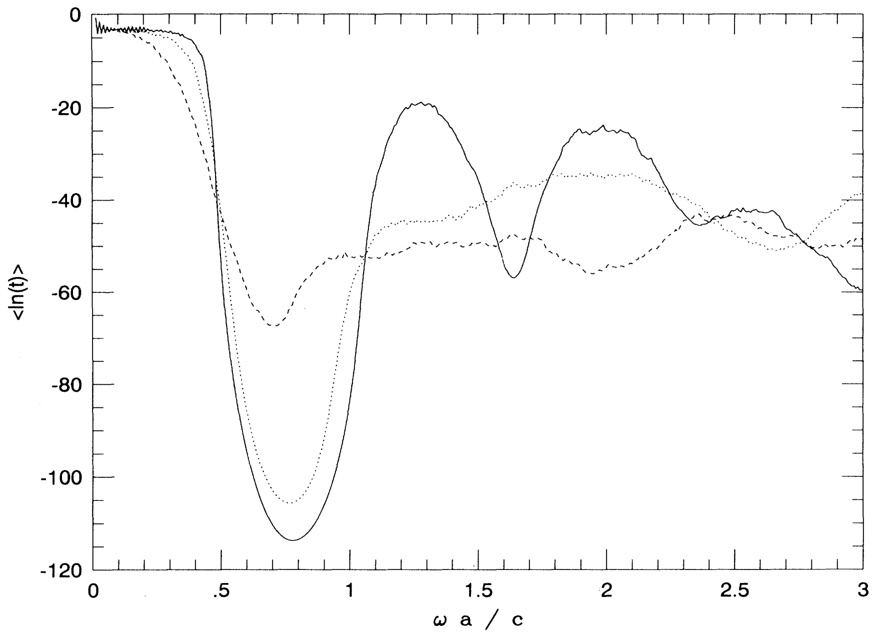

FIG. 6. $\langle \ln(t) \rangle$ vs $\omega a/c$ for a system similar to that used in Fig. 4 consisting of 40 bilayers with thickness error 20, 40, and 80% (solid, dotted, and dashed lines) in each layer and $\theta=0°$.

terial[19–21] are shown in Table I. In all three cases, $\langle \ln(t) \rangle$ has a drop at low frequencies which corresponds to the first gap of the corresponding periodic case and its exact location depends on the particular materials consisting the multilayer, while for high frequencies, $\langle \ln(t) \rangle$ saturates to a constant value. Using Eq. (7), we can calculate the localization length which corresponds to this saturated value of the average transmittance; in particular, the localization length is $9a$, $6.2a$, and $3.6a$ for Al, Si, and Cd, respectively, as the second material; a is the average thickness of each bilayer. Al and lucite have the smaller density and velocity ratios and the higher saturated values for the localization length, while for Cd and lucite the density and velocity ratios are much higher and the saturated value of the localization length is about 2.5 times smaller than this of the Al and lucite system. For steel and lucite (see Fig. 4), l is almost equal to $2a$, so this system is the best candidate for the experimental observation of elastic-wave localization. In fact, recently reported was an observation of the localization of bending waves in a thin steel plate decorated with lucite blocks forming a 2D square lattice.[22] The present results seems to support that observation, although, as noted by the authors, the disorder is probably related to the change of the properties of lucite close to the connections with steel rather than a disorder in the volume of the lucite blocks;

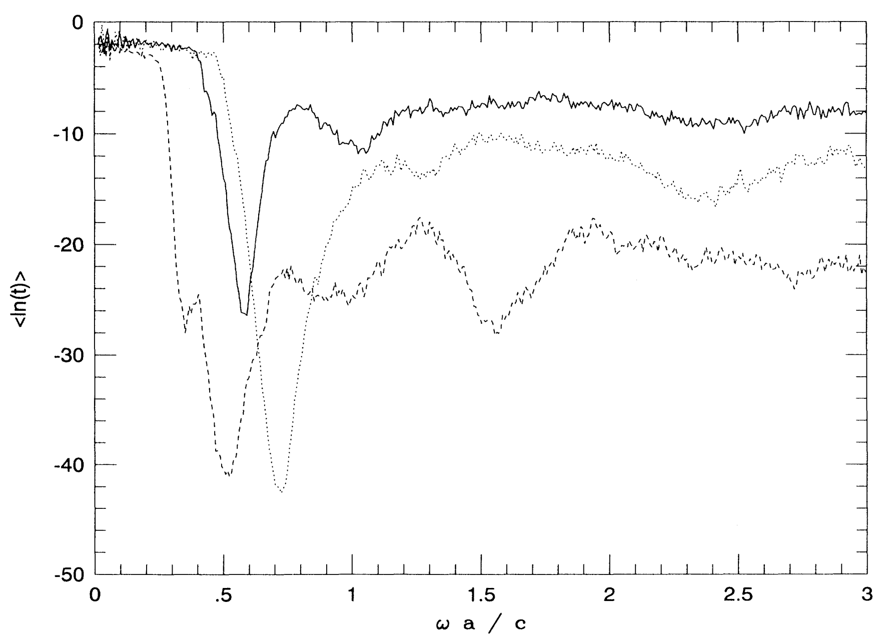

FIG. 7. $\langle \ln(t) \rangle$ vs $\omega a/c$ for a 40-bilayer disordered system with thickness error 40% in each layer and $\theta=45°$; in all the cases one of the layers is lucite, while the other one is Al, Si, or Cd (solid, dotted, and dashed lines); the average thickness of each layer is $a/2$.

also the geometry and the underlying equations are different. Finally, the present results, which show that for any incident angle, the localization length becomes smaller as the density and velocity contrasts become higher, further support the statement that bubbles inside a liquid are a very favorable system for the study of the localization of acoustic waves, since the ratios of density and sound velocities in that system are extremely high (this statement has been reached by studying a periodic arrangement of air spheres in a liquid[23,24]); note that for $\theta=0°$ the present results for the elastic waves are directly applied to the corresponding case of the propagation of acoustic waves through fluids multilayers.

In order to check how the average transmission depends on the incidence angle, we examine $\langle \ln(t) \rangle$ for high amount of disorder and high frequencies; in that case, as we explained previously, $\langle \ln(t) \rangle$ saturates to an almost constant value $\langle ln(t) \rangle_c$. For a 40-bilayer system consisting of equal, on average, thickness steel and lucite plates and assuming 80% thickness error, $\langle \ln(t) \rangle_c$ is -50 and -43 for $\theta=0°$, 45° respectively. Also, our calculations show that for θ greater than about 30°, $\langle \ln(t) \rangle_c$ is almost independent of θ, while for smaller θ, $\langle \ln(t) \rangle_c$ increases slowly by increasing θ. The velocity contrast for L-type of waves (Table I) is 1.48, while the velocity contrast for T-type of waves is smaller (1.13), so, L-type of waves tend to be more localized; also, as we noted earlier, for $\theta=0°$, only the L-type of waves are excited, while for $\theta\neq0°$ both L- and T-type of waves are excited; for that reason we expect that for $\theta=0°$, the $\langle \ln(t) \rangle_c$ and the corresponding localization length will be smaller.

VI. ABSORPTION

In general, the presence of structural damping, represented by a loss factor, would make the Young modulus E and hence c_L, c_T would be complex.[19] In the following section, we present results for a multilayer consisting of steel and lucite plates in which E for the lucite is complex with a constant (independent of frequency) imaginary part, while E for the steel is real since the losses for steel are much smaller than lucite.

Figure 8 shows the $\ln(t)$ vs $\omega a/c$ for a periodic bilayer consisting of equal thickness steel and lucite plates embedded in water; the incident angle is 45° and the imaginary part of the Young modulus of lucite is $E_i=100$ kbar. The main effect of the absorption is that the transmission becomes thickness dependent for every frequency, e.g., the transmission obeys the following relation: $\ln(t)=-2\Lambda/l_a$, where l_a is the frequency-dependent absorption length; this is clearly shown by comparing the transmission results for the 20- and 40-bilayer cases (compare solid and dotted lines in Fig. 8).

The effect of the absorption can be also studied by changing the value of E_i. Figure 8 shows the $\ln(t)$ vs $\omega a/c$ for a 40-bilayer system consisting of equal thickness steel and lucite plates using two different values for the imaginary part of the Young modulus of lucite: $E_i=100$ and 200 kbar (dotted and dashed lines in Fig. 8). In general, the effect of the absorption increases as a function of frequency although there are some exemptions. In particular, for frequencies inside the first and fourth gap at $\omega a/c$ around 0.55 and 1.65, respectively, the transmission is almost the same or it is getting even higher by increasing E_i. But even outside of the gaps, there are frequency regions where the effect of the absorption is more prominent than for higher-frequency regions; for example at $\omega a/c=0.9$, $\ln(t)$ is -40, -75 for $E_i=100$ and 200 kbar, respectively, while at $\omega a/c=1.2$, it is -17, -27 for $E_i=100$ and 200 kbar, respectively. Also, the absorption is extremely high at $\omega a/c$ around 2.5.

For an homogeneous lucite plate, the displacement is proportional to $\exp(i\omega y/c)$; since E is complex the wave vectors and the sound velocities are complex, so, we actu-

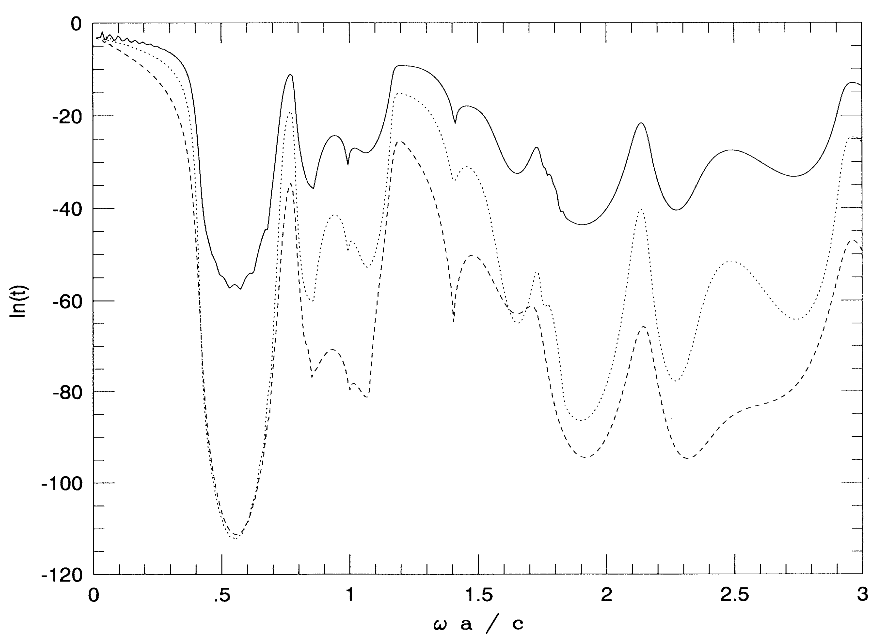

FIG. 8. $\ln(t)$ vs $\omega a/c$ for an N-bilayer periodic system consisting of equal thickness steel and lucite plates; the Young modulus of the lucite has an imaginary part, E_i, and $\theta=45°$; $E_i=100$ kbar, $N=20$ (solid); $E_i=100$ kbar, $N=40$ (dotted); $E_i=200$ kbar, $N=40$ (dashed).

ally expect the general trend to be that the effect of the absorption is more prominent as the frequency increases. The deviations from that general trend are caused by the nonhomogeneous nature of the system; in that case, we expect that the effect of the absorption will be more prominent when the displacement vectors have maximum amplitudes at the high absorptive lucite plates and this seems to be the case for $\omega a/c$ around 0.9 and 2.5. Finally, the small oscillations in the transmission due to the multiple scattering between the two boundaries of the system, which are more obvious at small frequencies [see Fig. 1(c)], disappear with the introduction of the absorption.

We have also studied the effect of the absorption in the presence of disorder and how the physical picture presented in the previous section changes with the addition of dissipation. Figure 9 shows the $\langle \ln(t) \rangle$ vs frequency for a 40-bilayer system consisting of steel and lucite plates of equal, on the average, thickness embedded in water and assuming an $\theta=0°$ incident angle; $\langle \ln(t) \rangle$ has been calculated by averaging over 100 configurations, the thickness errors for each plate are 20 and 40 % and the E_i of the lucite is 100 kbar. Comparing the absorbing cases (Fig. 9) with the nonabsorbing ones (Fig. 6), we find that $\langle \ln(t) \rangle$ is smaller for the absorbing cases and this effect become more obvious as the frequency increases; there is an exception in that general trend for $\omega a/c$ around 0.8, in which there is a sharp drop in the average transmission, the remnant of the first gap of the periodic case.

As we discussed in the previous section, the average transmission of a disordered multilayer is thickness dependent: $\langle ln(t) \rangle = -2\Lambda/l$. Similarly, as we showed in the beginning of this section, the transmittance of a periodic multilayer is thickness dependent in the presence of absorption: $\ln(t) = -2\Lambda/l_a$. It has been suggested that in the presence of both disorder and absorption the average transmittance is given by the expression:[6] $\langle ln(t) \rangle = -2\Lambda(1/l + 1/l_a)$. The previous expression suggests that for any amount of disorder and for the same amount of absorption, the difference Δ between the transmittance of the absorbing and the nonabsorbing cases is $\Delta = -2\Lambda/l_a$, which is independent of the amount of disorder. In Fig. 10, we check the validity of the previous statement for the same system as that of Fig. 9 and for three different thickness errors: 20, 40, and 60 %. Δ is almost independent of the amount of disorder for frequencies $\omega a/c$ below 0.35; note that this frequency region corresponds to the lower edge of the first gap of the periodic case and this is the same region considered in Ref. 6. But, for higher frequencies, there are considerable differences between the Δ for different amount of disorder, although, for the 40 and 60 % errors the differences are much smaller. For the 20% thickness error, Δ has a drop at $\omega a/c$ around 0.9 and a smaller one at around 2.5; this is an indication that the effect of the absorption is higher at those frequencies. Note that these are also the frequency regions where the absorption is higher in the corresponding periodic case (see Fig. 8), so, the same argument regarding the maxima of the displacement vector can be also applied in the present low disorder case. On the other hand, for a high amount of disorder this argument cannot be used anymore. We can see that by considering the extreme case of 100% error thickness; in that case, the maxima of the displacement have the same probability, on the average, to be on the highly absorbing lucite plates as well as in the nonabsorbing steel plates, so, on the average, the effect of the absorption will be similar to that of the homogeneous absorbing plate. This is fully confirmed by the results in Fig. 10, which shows that for a high amount of disorder, Δ tends to an almost straight line, which monotically decreases by increasing the frequency.

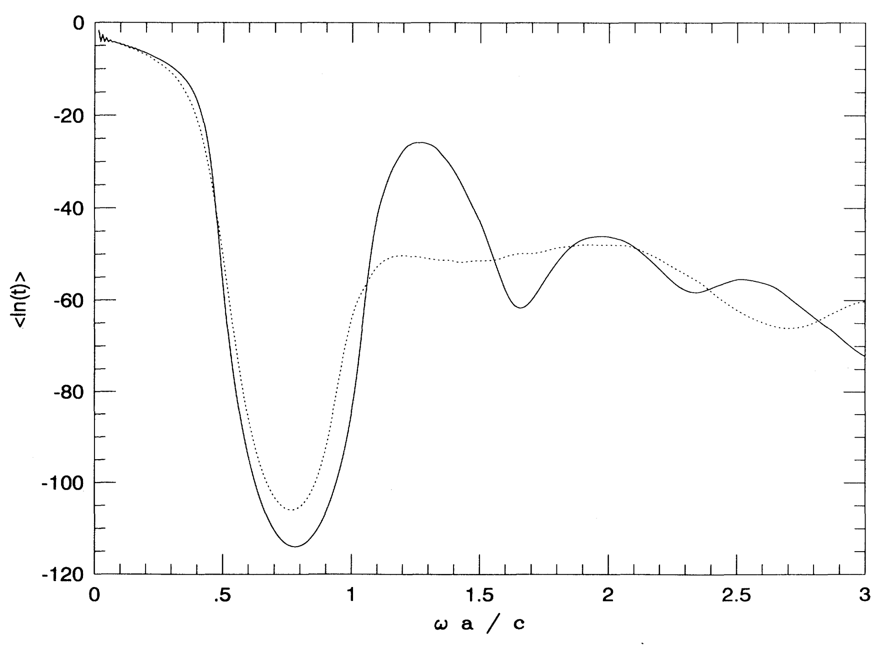

FIG. 9. $\langle \ln(t) \rangle$ vs $\omega a/c$ for a disordered system of 40 bilayers similar with that described in Fig. 6 assuming 20 and 40 % thickness error (solid and dotted lines) for each layer; the imaginary part of the Lucite's Young modulus is $E_i = 100$ kbar and $\theta=0°$.

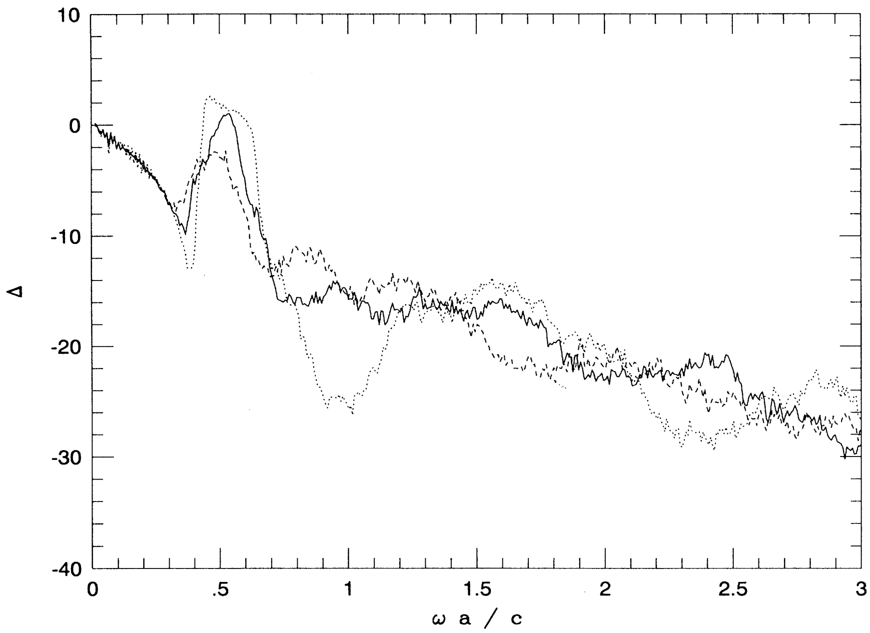

FIG. 10. The difference, Δ, between the transmission of the absorbing and nonabsorbing disordered systems similar with those described in Figs. 6 and 9 with 20, 40, and 60 % (dotted, solid, and dashed lines) thickness error in each layer; in the absorbing cases, the imaginary part of the Young modulus is $E_i = 100$ kbar and $\theta = 45°$.

VII. CONCLUSIONS

We have made a systematic study of elastic-wave propagation through solid multilayers. We used the periodic bilayer system as the starting point. In that case, the transmission profiles has substantial differences between normal and non-normal incidence due to the fact that even for small deviations from $\theta = 0°$, both longitudinal and transverse type of waves are excited in contrast with the $\theta = 0°$ case where only one type of wave can be excited. We have showed that this may cause problems if one wants to construct wide stop-band filters (corresponding to the gaps of the periodic solid multilayers) or narrow band-pass filters (constructed by introducing defects in an otherwise periodic solid multilayer) operated in a wide range of incidence angles. Those problems can be avoided by carefully choosing multilayers where the gaps of the *L*- and *T*-type waves overlap in a wide range of incidence angles.

By introducing an error in the thickness of each layer, the average transmission of the disordered multilayer become thickness dependent ($\langle \ln(t) \rangle = -2\Lambda / l$, where l is the so-called localization length) for every frequency, in contrast with the corresponding periodic cases where the transmission is thickness dependent [$\ln(t)$ is proportional to $-\Lambda$] only for frequencies inside the gaps. The first gap of the periodic case survives even for a high amount of disorder, while the other higher gaps of the periodic case disappear quickly with the application of the disorder; by increasing the disorder, $\langle ln(t) \rangle$ increases for frequencies inside the first gap of the periodic case because the density of states increases. For ω approaching 0, l increases, while for high frequencies l saturates to a constant value l_s which is independent of frequency; however, l_s strongly depends on the velocity and density ratios between the two materials constructing the disordered multilayer. In particular, l_s is about $2a$ for steel and lucite where both velocities and densities contrasts are high, while l_s is about $9a$ for Al and lucite where both velocities and density contrasts are small.

In the presence of absorption, the transmission of a periodic multilayer becomes thickness dependent [$\ln(t) = -2\Lambda / l_a$ where l_a is the absorption length] for every frequency, while there are certain frequency regions where the effect of the absorption is more prominent. Finally, we have checked the relation $\langle \ln(t) \rangle = -2\Lambda(1/l + 1/l_a)$, which has been proposed in the presence of both absorption and disorder; for a small amount of disorder, this formula works only for low frequencies, while for a high amount of disorder holds for every frequency.

ACKNOWLEDGMENT

Ames Laboratory is operated by the U.S. Department of Energy by Iowa State University under Contract No. W-7405-Eng-82.

[1] *Scattering and Localization of Classical Waves in Random Media*, edited by P. Sheng (World Scientific, Singapore, 1990).

[2] *Photonic Band Gaps and Localization*, Vol. 308 of *NATO Advanced Study Institute, Series B: Physics*, edited by C. M. Soukoulis (Plenum, New York, 1993).

[3] S. John, Phys. Rev. Lett. **58**, 2486 (1987).

[4] J. M. Frigerio, J. Rivory, and P. Sheng, Opt. Commun. **98**, 231 (1993).

[5] P. Sheng, B. White, Z.-Q. Zhang, and G. Papanicolaou, in *Scattering and Localization of Classical Waves in Random Media* (Ref. 1), p. 563; Phys. Rev. B **34**, 4757 (1986).

[6] A. R. McGurn, K. T.Christensen, F. M. Mueller, and A. A.

Maradudin, Phys. Rev. B **47**, 13 120 (1993).
[7]A. Kondilis and P. Tzanetakis, Phys. Rev. B **46**, 15 426 (1992).
[8]L. M. Brekhovskikh, *Waves in Layered Media* (Academic, New York, 1960).
[9]W. M. Ewing, W. S. Jardetsky, and F. Press, *Elastic Waves in Layered Media* (McGraw-Hill, New York, 1967).
[10]R. E. Camley, B. Djafari-Rouhani, L. Dobrzynski, and A. A. Maradudin, Phys. Rev. B **27**, 7318 (1983).
[11]B. Ursin, Geophysics **48**, 1063 (1983).
[12]B. G. Martin, J. Acoust. Soc. Am. **91**, 1469 (1992).
[13]D. Levesque and L. Piche, J. Acoust. Soc. Am. **92**, 452 (1992).
[14]M. L. Munjal, J. Sound Vib. **162**, 333 (1993).
[15]J. P. Dowling, J. Acoust. Soc. Am. **91**, 2539 (1992).
[16]R. Esquivel-Sirvent and G. H. Cocoletzi, J. Acoust. Soc. Am. **95**, 86 (1994).
[17]P. J. Shull and D. E. Chimenti, J. Acoust. Soc. Am. **95**, 99 (1994).
[18]V. K. Kinra, P. T. Jaminet, C. Zhu, and V. R. Iyer, J. Acoust. Soc. Am. **95**, 3059 (1994).
[19]L. Cremer and M. Heckl, *Structure-Borne Sound* (Springer-Verlag, Berlin, 1988).
[20]O. L. Anderson, in *Physical Acoustics III B,* edited by W. P. Mason (Academic, New York, 1965), p. 43.
[21]W. P. Mason, *Physical Acoustics and the Properties of Solids* (Van Nostrand, New Jersey, 1958).
[22]L. Ye, G. Cody, M. Zhou, P. Sheng, and A. N. Morris, Phys. Rev. Lett. **69**, 3080 (1992).
[23]M. M. Sigalas and E. N. Economou, J. Sound Vib. **158**, 377 (1992).
[24]E. N. Economou and M. M. Sigalas, Phys. Rev. B **48**, 13 434 (1993).